Journal of Petroleum Science and Engineering 167 (2018) 654–663

Contents lists available at ScienceDirect

Journal of Petroleum Science and Engineering

journal homepage: www.elsevier.com/locate/petrol

Performance of CO_2 flooding in a heterogeneous oil reservoir using autonomous inflow control

Haavard Aakre[a,b,*], Vidar Mathiesen[b], Britt Moldestad[a]

[a] University of Southeast Norway, Norway
[b] Inflowcontrol, Norway

ABSTRACT

CO_2-EOR is one of the main methods for enhanced oil recovery. The injection of CO_2 does not only improve oil recovery, but also contributes to reduction of greenhouse gas emissions. However, many CO_2-EOR project are reporting problems with breakthrough and reproduction of CO_2, which results in poor distribution of CO_2 in the reservoir. This paper analyzes the world first trial test for the autonomous inflow control valves in a CO_2-EOR oil reservoir. The autonomous flow control valves can choke back unwanted fluid such as pure water, gas, carbonized water and pure CO_2. Choking back the breakthrough zones, will increase the reservoir area exposed for CO_2 and increase the oil recovery. The trial well was originally an open hole well and has been recompleted with inflow control and packers. The packers are installed to isolate the well in three different zones. The autonomous inflow control valves (AICVs) do not require any external connection or force and this makes the valves simple and robust. The valves will locally choke or close in the zones with high water or gas production, and simultaneously produce more from the zones with high oil saturation. The production with autonomous inflow control valves is compared to the historical production data from the open-hole well. Performance curves for oil, water and gas are presented. The trial tests show that the autonomous inflow control valve chokes back unwanted fluid such as pure water, carbonized water and supercritical CO_2, and due to this, the drawdown can be increased resulting in increased oil production.

Simulations were performed with NETool, which is a steady state one dimensional near well simulation tool. Simulations were run using the trial well data and the reservoir conditions from the Midale field. An autonomous inflow control model implemented in NETool was tuned to fit the performance curves for the AICV. Relative permeability curves for carbonate reservoirs was estimated and implemented in NETool. Simulations were performed with passive inflow control devices (ICDs) and autonomous inflow control valves (AICVs). The results indicate that the oil production can be increased with more than 400% when AICV is used at high drawdown. ICD cannot choke locally for water or CO2, and is producing very high amount of unwanted fluids at high drawdown. The water cut using AICV is 65% at 50 bar drawdown whereas the water cut is close to 100% when using ICD. Results from simulations are compared to production data, and NETool was able to predict the potential of increased oil recovery with AICV completion well.

1. Motivation

Injection of CO_2 to oil reservoirs is one of the most utilized methods for enhanced oil recovery (EOR). In addition to increasing the total oil production from a field, CO_2 EOR can be used in combination with CO_2 storage to mitigate CO_2 emissions. The method is widely used in the United States and Canada. InflowControl AS has developed an autonomous inflow control valve, AICV, which can avoid direct reproduction of CO_2 to the well in fields using CO_2 injection. A vertical well with AICV completion is installed in the Midale field, Canada. The field has CO_2 injection, and the functionality of the AICV regarding closing for water and CO_2 is tested. Many CO_2-EOR projects are reporting problems with breakthrough and reproduction of CO_2. This results in a poor distribution of CO_2 in the reservoir, and parts of the field will not be exposed for CO_2. Choking back the breakthrough zones where the reproduction of CO_2 occurs will give a better distribution of CO_2 in the reservoir and increase the oil recovery. Closing the breakthrough zones, will contribute to reduce the required amount of injected CO_2, reduce the demand of separation systems and thereby reduce costs and energy demand.

* Corresponding author. University of Southeast Norway, Norway.
E-mail address: haavard.aakre@inflowcontrol.no (H. Aakre).

https://doi.org/10.1016/j.petrol.2018.04.008
Received 14 November 2017; Received in revised form 23 March 2018; Accepted 4 April 2018
Available online 05 April 2018

2. CO_2 EOR

The efficiency of CO_2 injection for EOR is dependent on the miscibility of CO_2 in oil (U.S. Department of Energy, 2015). When CO_2 is injected into an oil reservoir, light hydrocarbons from the oil dissolve in the CO_2 and CO_2 dissolves in the oil. This occurs most readily when CO_2 is compressed and when oil is containing a considerable volume of light hydrocarbons. When CO_2 dissolves in oil, the viscosity of the oil decreases significantly. The reduction of oil viscosity is highly dependent on the initial viscosity of the oil. Less viscous oil will be less affected by the CO_2, while for more viscous oils, the effect of viscosity reduction is more pronounced. The reduction in oil viscosity will cause an increase in the oil relative permeability and mobility. This will reduce the residual oil saturation in the reservoir and improve the oil recovery (Zhang et al., 2015). CO_2 interacts with the oil in the reservoir and dissolves in the oil at certain reservoir conditions. The dissolution of CO_2 in oil causes the oil to swell. Reservoir characteristics, as pressure and temperature as well as oil composition, determine the strength of the oil swelling effect (Zhang et al., 2015). Swelling plays an important role in achieving better oil recovery. Variations in the swelling factor influences on the residual oil saturation, which is inversely proportional to the swelling factor. Residual oil saturation, in turn, affects the relative permeability, which plays a crucial role in oil recovery (Zhang et al., 2015). Swollen oil droplets force fluids to move out of the pores and oil that initially was unable to produce will now be forced to move towards the production well. Hence, oil swelling causes drainage effect that decreases the residual oil saturation (Zhang et al., 2015). An oil reservoir also contains disconnected pores. Swelling of the oil can contribute to additional oil recovery by reconnecting the disconnected pores (Zhang et al., 2015). Swelling of oil is assumed proportional to the solubility of CO_2 in the oil. Experimental research has been performed with 821 and 9.7 cP oils to investigate the swelling of oil saturated with CO_2. It was found that the saturated swelling factors were 1.12 and 1.25 for the 821 and 9.7 cP oil respectively (Optimization of CO2).

Mobility ratio, M, is the ratio between water/oil volumetric flow rates. It depends on viscosity and permeability of water and oil phases. The mobility ratio is expressed by:

$$M = \frac{k_{rw}}{k_{ro}} \cdot \frac{\mu_0}{\mu_w} \quad (1)$$

where μ is the dynamic viscosity, k_r is the endpoint relative permeability and the subscripts o and w indicate the oil and water phases respectively. The endpoints are the residual oil saturation and the irreducible water saturation. Injection of CO_2 changes the relative permeability curves by changing the endpoints and the shape of the curves. In addition, the viscosity of oil will decrease, and all together, this results in reducing the mobility ratio. The oil recovery efficiency increases with decreasing water-oil mobility ratio.

CO_2 injection is often used in carbonate reservoirs. Carbonate reservoirs has usually low permeability, but very often, the reservoirs contains zones with high permeability and fractures. Due to high permeability zones and fractures, EOR schemes utilizing CO_2 alternating water injection often experience significant problems and challenges with short circuiting of CO_2 gas and water between injectors and producers, and thereby significant amounts of oil is left behind. This is illustrated in Fig. 1. Choking back the breakthrough zones where the reproduction of CO_2 occurs will give a better distribution of CO_2 in the reservoir (Fig. 2), increase the oil recovery and reduce the required amount of injected CO_2. The redistribution of the injected fluid after choking back the breakthrough zone are dependent on the zonal isolation along the well. Packers are used to avoid crossflow in the annulus. If the reservoir has a major crossflow between the different layers, the fluid will bypass the packers through the reservoir and the zonal isolation will be difficult and result in a poorer redistribution of the injected fluid.

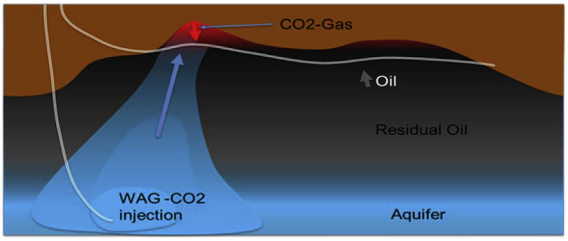

Fig. 1. Illustration short circuiting of CO_2 gas and water between injector and production well.

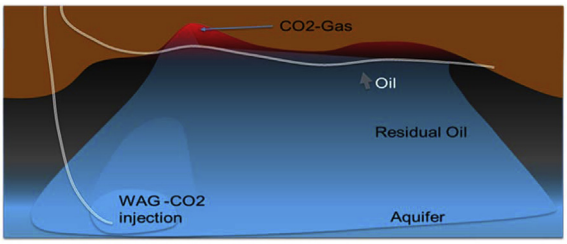

Fig. 2. Illustration of improved distribution of CO_2 in the reservoir by choking back the breakthrough zone.

Fig. 3 shows the production history of the Midale field, and the increased oil recovery due to CO_2 injection. In 2014, efforts were done to improve the oil recovery further, and the efforts succeeded by reducing oil declines, increasing oil production and reducing costs associated with injection quantities. However, further improvements were possible by utilizing inflow control technology, and the world's first field trial of the AICV in a water and CO_2 injection scheme, and the world's first comparison with conventional ICD technology in the same well were started (Kais et al., 2016). The AICV technology opens up for increasing the drawdown and thereby increasing the production rates if wanted. The AICV has to be designed based on the properties in the specific reservoir. Closing off the flow of CO_2 or carbonated water to the production well and getting a better distribution of CO_2 in the reservoir, also contributes to storage of CO_2 in the reservoir during the period of oil production. To choke back the breakthrough zone the AICV technology need to have some difference in viscosity or density in order to differentiate the flow through for the different fluids. However, water has usually lower viscosity than oil. CO_2 gas has always lower viscosity than oil and water. For oil and water with equal viscosity the density difference is sufficient for the technology to differentiate between the phases. The installation of an AICV well is usually done with sand screens and packers, the same way as for ICD well. The packers in the AICV well will be exposed to higher differential pressure than the ICD well, due to the choking of the breakthrough zone. This requires packers that can resist the high-pressure differences.

3. AICV technology and design for CO_2 EOR in Midale

The AICV has the feature to distinguish between fluids, based on fluid viscosity and density, and the AICV design is adapted to the conditions and requirements in the relevant field. The functionality of the AICV, which is to keep open for high viscous fluids like oil, and to close for fluids like water and gas, is based on the difference in the pressure drop in a laminar flow element compared to a turbulent flow element as illustrated in Fig. 4. The main flow enters a conduit, A, at inlet pressure P1 (reservoir pressure). The pilot flow is passing through a laminar flow element where a pressure drop occurs and the pressure is reduced to P2. The flow is further flowing through the turbulent flow element before it exits the flow conduit at the well pressure, P3. The fluid properties and flow rate of the pilot flow determine the pressure,

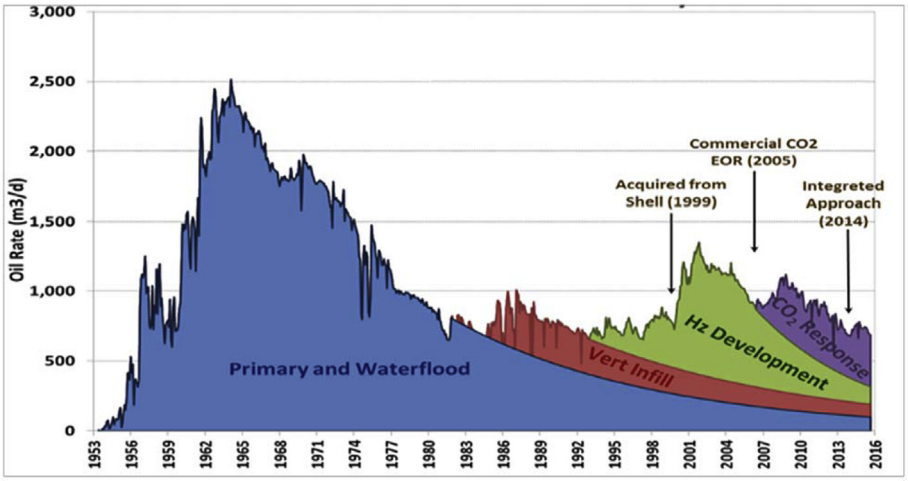

Fig. 3. Midale production history and production response since the 2014 integrated approach (Kais et al., 2016).

P2, which is the pressure controlling the valve functionality. The AICV is designed to let approximately 99% of the total flow go through the main flow and the rest through the pilot flow. When the valve is closed, the minor pilot flow represents the total flow rate through the valve.

The laminar flow element (LFE) can be considered as a pipe segment and the pressure drop is expressed as:

$$\Delta p = f \cdot \frac{L.\,\rho.\,v^2}{2.D} = \frac{64}{\mathrm{Re}} \cdot \frac{L.\,\rho.\,v^2}{2.D} = \frac{32.\mu.\,v.\,L}{D^2} \tag{2}$$

where f is the laminar friction factor $\left(\frac{64}{\mathrm{Re}}\right)$, ρ is the fluid density, μ is the fluid viscosity, ν is the fluid velocity, L and D is the length and diameter of the laminar flow element respectively. The pressure drop through the pipe segment is proportional to the fluid viscosity and the velocity. The turbulent flow element (TFE) can be considered as a thin plate orifice. The pressure drop through an orifice is given by:

$$\Delta P = k \cdot \frac{\rho \cdot v^2}{2} \tag{3}$$

where k is a geometric constant. The pressure drop through the turbulent restrictor is proportional to the fluid density and the velocity squared. The lower plot in Fig. 4 shows the pressure at different positions along the pilot flow path for oil, gas and water, respectively. When the pressure drop through the laminar flow element is high, as for oils, P2 is low and the valve will stay in open position producing oil. When low viscous fluids flow through the LFE, the pressure drop is low, and the pressure in B is high. The high pressure will actuate a piston, and the valve will close. Fig. 5 illustrates the AICV in **open and closed position.**

The force balance around the piston is controlling the piston position, as shown in Fig. 6. The force, F1, on the upper part of the piston (P1·A1) is acting downwards and the force F2 below the piston (P2·A2) is acting upwards. F_{fric} is a friction force, which will work against the direction of fluid flow. F_{fric} will mostly be normal to F1, F2 and F3. F3 is acting downwards on the outer part of the piston. Most of the pressure drop of the main flow is located at the smallest passage, between the piston and the seat. The size of this opening will define the ICD strength of the AICV. When the net force (F1-F2 + F3 ± F_{fric}) is positive, the valve is in open position and if the net force is negative, the valve

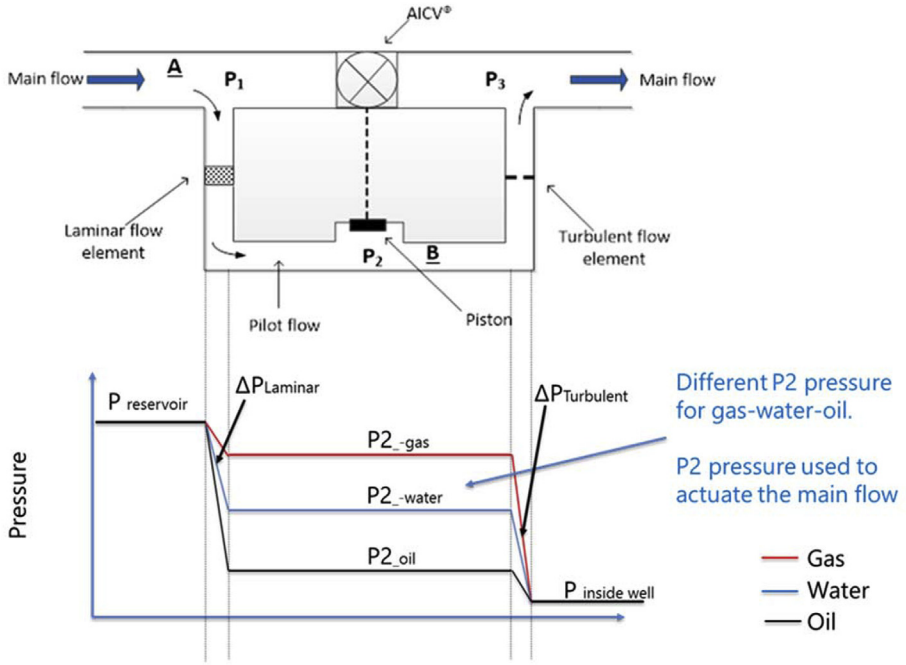

Fig. 4. The pressure drop through a combination of laminar and turbulent flow restrictors in series.

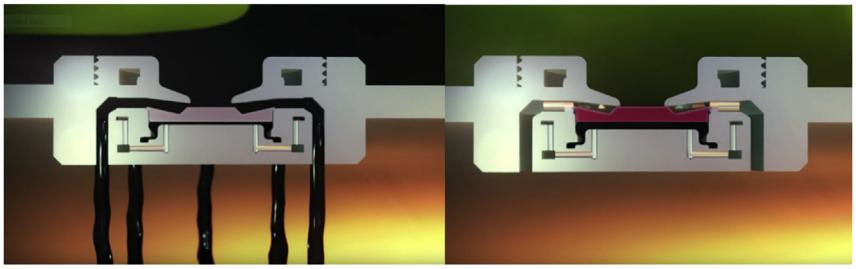

Fig. 5. AICV in open and closed position.

closes. The ratio between A1 and A2 is a design parameter and the optimum ratio is dependent on the properties of the oil, gas and/or water.

The AICV technology is described earlier (Mathiesen et al., 2014; Aakre et al., 2013a, 2013b, 2014; Kais et al., 2016).

A vertical well with AICV completion is installed in the Midale field in Saskatchewan. The reservoir is perforated in three sets at three different depths. The vertical well includes two AICVs in each of the three perforated zones, i.e. totally six AICVs. The Midale field is a heterogeneous field, and due to differences in permeability, the production rates from the three zones differ significantly. One of the perforated zones has high production rates whereas the other two have low rates. The advantage of AICV is that the same design can be used for all the three production zones, as long as the valves are designed to close or choke for unwanted fluids. Packers are installed to isolate the zones and avoid annulus flow from one zone to another. Fig. 7 shows an AICV mounted in a base pipe with sand-screen.

The AICV used in this project, is designed to keep open for oil and choke for supercritical CO_2 and water. Water has a higher viscosity than CO_2, which implies that if the valve is designed to choke for water, it will also close for CO_2. The most important design parameter for the AICV functionality is the oil/water viscosity ratio. The viscosity ratio in the near well area for the actual field is about 6.5, which is an acceptable ratio to give a good oil/water/CO_2 separation. The higher viscosity ratio there is the easier to design an AICV to close for water and CO_2 and keep open for oil. The design is also based on flow rates as a function of pressure drop over the AICV. The flow rates are specified by the customer and are based on the reservoir and fluid properties. An AICV for the Midale field is constructed and tested.

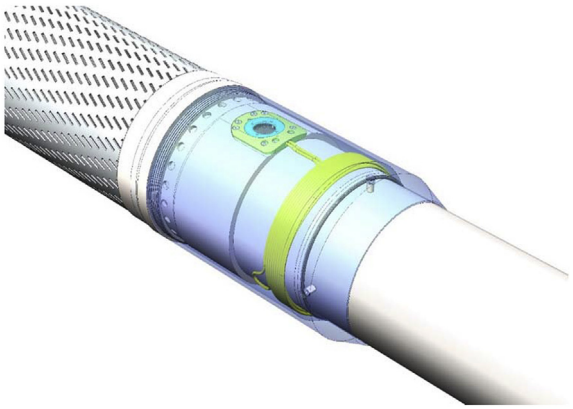

Fig. 7. AICV mounted in the base pipe with sand screen.

4. Production data from the Midale field

Kais et al. (2016) have published the results of the world's first field trial of the AICV in a water and CO_2 injection scheme, and a selection of the results from the trial well with AICV are presented here. The focus was to increase the oil production as much as possible, and therefore the total liquid flow should be kept high. The average liquid and oil production rates before the recompletion of the well were 1100 bpd and 5 bopd respectively. The production had to be run with a low drawdown to avoid the total flow to exceed the capacity of the production and separation system. Table 1 presents the performance data for the trial candidate well before installation of inflow control completion.

The well with ICD and AICV completion was tested and the results were compared to the results without inflow control. When using AICV completion, the drawdown can be increased and more oil can be

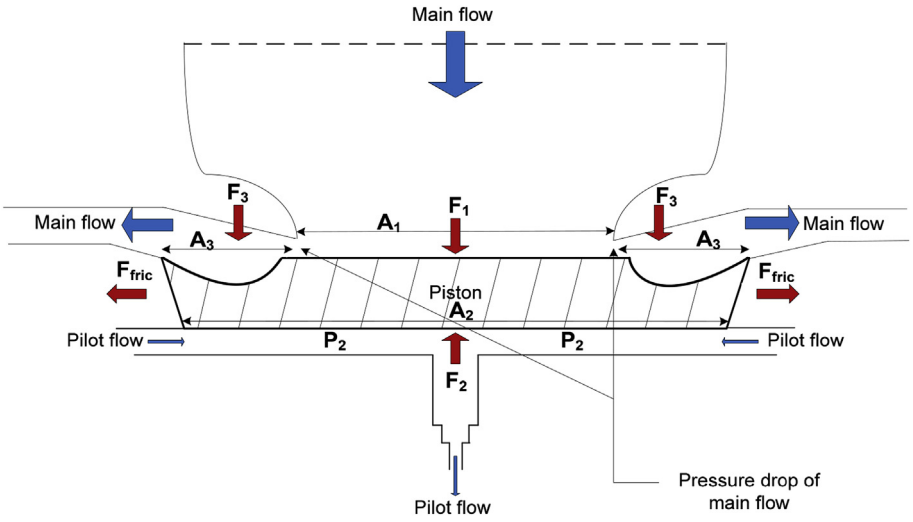

Fig. 6. The areas and forces acting on the AICV piston.

Table 1
Well performance summary of trial well (Kais et al., 2016).

Results Summary	Comparison vs Baseline	Highest Rates		Averages					
		Liquid	Oil	Liquid	Oil	GOR	THP	Oil Cut	Water
		bpd	bopd	bpd	bopd	scf/bbl	Kpa	%	%
BaseLine: Commingled in M1, M2 & M3 (No ICDs/AICVs)		2,050	10	1,100	5	32,000	7100	0.4	99.6

Table 2
Well performance summary – AICVs, data from (Kais et al., 2016).

Result summary	Highest rates		Averages					
	Liquid	Oil	Liquid	Oil	GOR	THP	Oil cut	WC
	bdp	bopd	bdp	bopd	Scf/bbl	kPa	%	%
Base line, no ICDs or AICVs	2050	10	1100	5	32,000	7100	0.4	99.6
ICD completion	3500	72	3500	45	10,500	3500	1.3	98.7
AICV completion	4800	57	3100	39	12,500	4400	1.3	98.5
Improvement	130%	460%	180%	690%	−60%	−40%	180%	−1.1%

produced from the low permeability zones M1 and M2. The tubing head pressure (THP) was decreased from 7100 kPa to 4400 kPa, which provides a corresponding increase in drawdown. The average oil rate increased from 5 to 39 bodp, which is an improvement of 690% on the oil rate. The summary of the results from the AICV and ICD completed wells is presented in Table 2. However, these results were poorer than expected for AICV most likely due to a damaged plug below the zone M3. Fluid from M3 was bypassing the AICVs and flew into the well via the damaged plug. Due to this, the main advantage of AICV (closing off the water production zone) did not appear in the results. However, the production from the low permeability zones can be assumed realistic.

5. Near well simulation of the trial well in the Midale field

The vertical trial well in the Midale field in Saskatchewan is simulated using the near well simulation tool NETool. NETool is a steady state near well simulation tool, and can be used to analyse the effect of different completion components, near-wellbore effect on productivity of the well, modelling of completion components in the production and injection interval, design of inflow control devices to delay water and gas breakthrough, etc. NETool can be linked with reservoir simulators such as Eclipse and Nexus, but this link is not used in this study. The Black-oil model is implemented in NETool, and is used in the simulations carried out in this study. The Black-oil model was used in this work, and is often used when limited specification about the reservoir fluids are available. The basic modelling assumption for the Black oil is that the gas may dissolve in the liquid oil phase, but no oil will dissolve in the gas phase. This implies that the composition of the gas phase is assumed to be the same at all pressures and temperatures (dwsim).

NETool can run simulations for various well completion designs, and one of the most important benefits of NETool is the ability to design and evaluate completion designs in a timely manner (NETool). This includes the evaluation of different types of passive and autonomous inflow control devices (ICDs and AICDs). NETool allows the user to modify the functions for ICDs and AICDs, and in that way, it is possible to adjust the functionality of the implemented types of AICD to also fit the functionality of AICV.

In this study, the reservoir conditions have been considered as steady state for the particular cases, and NETool has modelled the wellbore and completion hydraulics in detail. The input to NETool is reservoir conditions, fluid properties, and well design including annulus, pipeline, inflow control devices, screens and packers. The reservoir is specified by depth, porosity, saturation of the phases, permeability and relative permeability. The phase saturation, permeability and porosity can be specified for each zone.

There is no option to calculate relative permeability curves in NETool, so the user has to implement the current values. In this work, the Corey and Stone II correlations were used to calculate the relative permeability curves for water and oil. The Corey model is derived from capillary pressure data and is a good approximation for the relative permeability curves for water in a two-phase system. The relative permeability for water, k_{rw}, is given by:

$$k_{rw} = k_{rwoc}\left(\frac{s_w - s_{wc}}{1 - s_{wc} - s_{or}}\right) \tag{4}$$

where s_w is the water saturation, s_{wc} is the irreducible water saturation, s_{or} is the residual oil saturation, k_{rwoc} is the end point relative permeability for water at maximum water saturation, and n_{ow} is the Corey exponent. (Tiab and Donaldson, 2012).

The Stone II model is used to calculate the relative permeability of oil. The Stone II model estimates the relative permeability of oil in an oil-water system based on the following equation:

$$k_{row} = k_{rwoc}\left(\frac{s_w + s_{wc} - 1}{s_{wc} + s_{or} - 1}\right)^{n_{ow}} \tag{5}$$

where K_{row} is the relative oil permeability for the water-oil system, k_{rwoc} is the endpoint relative permeability for oil in water at irreducible water saturation and n_{ow} is a fitting parameter for oil. (Tiab and Donaldson, 2012) The irreducible water saturation is the maximum water saturation that a rock can have without producing water. Residual oil saturation represents the oil that cannot be produced by primary and secondary oil recovery. The exponents, n_w and n_{ow}, are functions of the pore size distribution in the reservoir, and typical values are n_w = 2–3 and n_{ow} = 6–8. (Ghoodjani and Bolouri, 2011) The oil and water saturation in the reservoir was specified for each zone. In addition fluid properties as viscosity and density are specified and used in combination with the Black-oil model.

Fig. 8 shows a principle sketch of the simulated vertical well and the location of the different production zones. The production zones are located below 1410 m depth. The sketch including well and production information are used as basis for NETool simulations. The different production zones (M1, M2 and M3) have different permeability, and most of the oil and water are produced from the high permeability zone, M3. In the simulations, the horizontal permeability is set to 5 mD in zone M1, 50 mD in M2 and 2000 mD in M3. The vertical permeability is 1/10 of the horizontal permeability. Since M1 and M2 have low permeability compared to M3, it is assumed that these two zones have still high saturation of oil, whereas M3 is almost 100% saturated with water. The oil saturation is set to 1.0, 0.9 and 0.0 for zone M1, M2 and M3

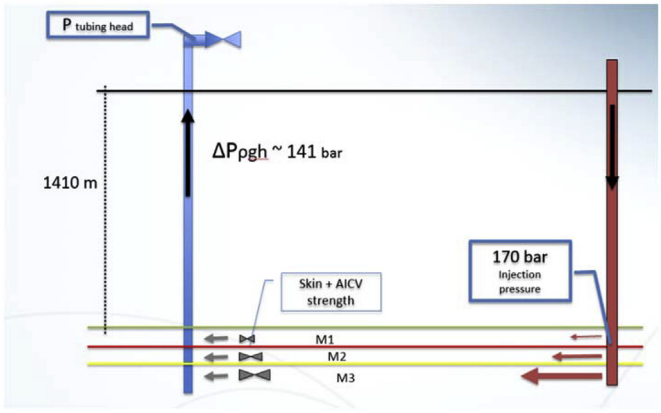

Fig. 8. Sketch of the vertical well used in the Midale field.

Table 3
Input data to NETool.

Reservoir parameters and well specification	Vertical well case	Units
Reservoir pressure	170	bar
Reservoir Temperature	75	°C
Oil viscosity	3	cP
Water viscosity	0.4	cP
Oil density	820	kg/m^3
Water density	1020	kg/m^3
Permeability M1: Horizontal/Vertical	5/0.5	mD
Permeability M2: Horizontal/Vertical	50/5	mD
Permeability M3: Horizontal/Vertical	2000/200	mD
Well length	10	m
Saturation in Zone 1: M1	$S_o = 1.0$, $S_w = 0.0$	–
Saturation in Zone 2: M2	$S_o = 0.9$, $S_w = 0.1$	–
Saturation in Zone 3: M3	$S_o = 0.0$, $S_w = 1.0$	–

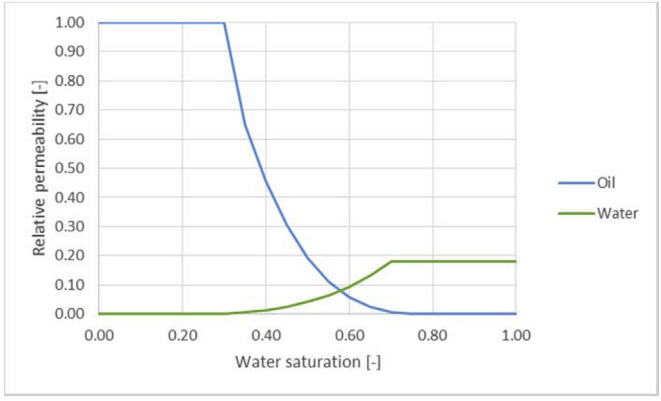

Fig. 9. Relative permeability curves for oil and water.

respectively. Table 3 presents the data used as input to NETool. The relative permeability curves are estimated based on Corey and Stone II, and is assumed to be influenced of the CO_2 injection. There are no available data on the relative permeability in the appropriate field. The Midale field is a carbonate field, and few data are available for this rock type. However, the rock type does not influence significantly on the relative permeability other than through the wetting preference (Schneider and Owens, 1970). In the simulations, the reservoir is assumed to be water-wet, and the relative permeability curves used are presented in Fig. 9. As zone M3 is 100% saturated with the water, the permeability will be the permeability for water and the relative permeability is 0.175. In zone M2, the reservoir is 90% saturated with oil, and regarding the relative permeability curves presented in Fig. 4, the permeability of oil will not be influenced by the water as long as the water saturation is lower than 0.3. This means that both in M2 and M3 the relative permeability of oil is 1. When CO_2 is injected into the reservoir, the permeability of oil and water changes as described in the introduction. The residual oil decreases, which means that more oil can be produced from the reservoir. This is taken into account by the relative permeability curves used in the simulation. The water phase is assumed as carbonated water, and the injection rate and mode of CO_2 injection are therefore not considered in the simulations. The simulations are steady state simulations, and the saturation of oil and water in the different zones is constant.

A model for Statoil's autonomous inflow control device called RCP [(Mathiesen et al., 2011; Halvorsen et al., 2012; Halvorsen (Statoil) et al., 2016)] is available in NETool and the user is allowed to specify the performance parameters for the RCP. The following equation describe mathematical function for the differential pressure as a function of volume flow through the RCP: [14, 16]

$$\delta P = f(\rho, \mu) \cdot a_{AICD} \cdot Q^x \tag{6}$$

$$f(\rho, \mu) = \left(\frac{\rho^2_{mix}}{\rho_{cal}}\right) \cdot \left(\frac{\mu_{cal}}{\mu_{mix}}\right)^y \tag{7}$$

$$f(\rho, \mu) = \left(\frac{\rho^2_{mix}}{\rho_{cal}}\right) \cdot \left(\frac{\mu_{cal}}{\mu_{mix}}\right) \tag{8}$$

$$\rho_{mix} = \alpha_{oil}\rho_{oil} + \alpha_{water}\rho_{water} + \alpha_{gas}\rho_{gas} \tag{9}$$

$$\mu_{mix} = \alpha_{oil}\mu_{oil} + \alpha_{water}\mu_{water} + \alpha_{gas}\mu_{gas} \tag{10}$$

where δP is pressure drop through the RCP, Q is the volume flow rate, x and y are user input constants, a_{AICD} is the valve strength parameter, α is the volume fraction of the actual phase, ρ_{cal} and μ_{cal} are the calibration density and viscosity respectively. The calibration fluid is most commonly water. The mixed viscosity and density are calculated based on the fraction of the different fluids in the mixture.

In the current case study, the RCP parameters are tuned to fit to the experimental performance behaviour for AICV. Fig. 10 represents the tuned curves for 3 cP oil and water. When tuning the oil performance curve, water at reservoir conditions with density 1020 kg/m^3 and viscosity of 0.4 cP was used as the calibration fluid. The tuning parameters x, y and a_{AICV} were found to be 2.42, 0.24 and $4.3 \cdot 10^{-5}$ respectively. The AICV is tuned to have an ICD strength of 2 bar, which means that the AICVs are producing 1 m^3 oil per hour at 2 bars differential pressure over the valve. The water viscosity used in the simulations is calculated by NETool and is based on the reservoir temperature and pressure. The performance curve for water is tuned by using the parameters x = 2.0, y = 1.1 and $a_{AICV} = 2.8 \cdot 10^{-5}$.

The simulations were performed with passive ICD and AICV, both with 2 bar strengths. The main objective of the simulations is to estimate the potential of increased oil production and decreased water

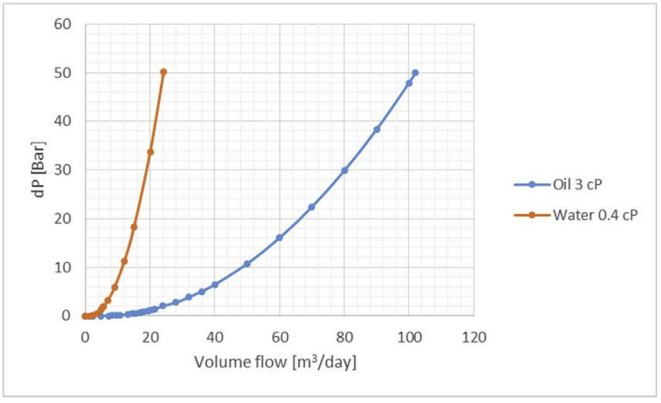

Fig. 10. Tuned performance curves for oil and water.

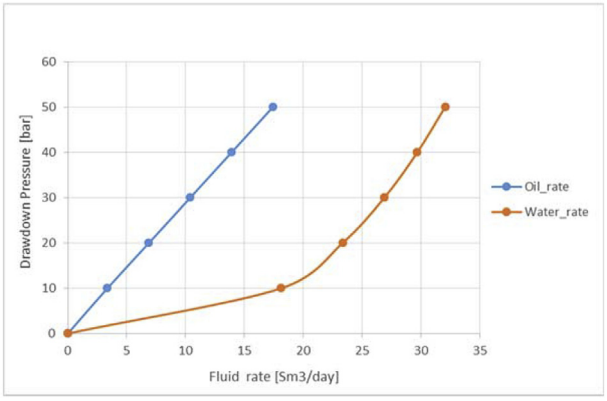

Fig. 11. Total production rates as a function of the drawdown pressure for AICV.

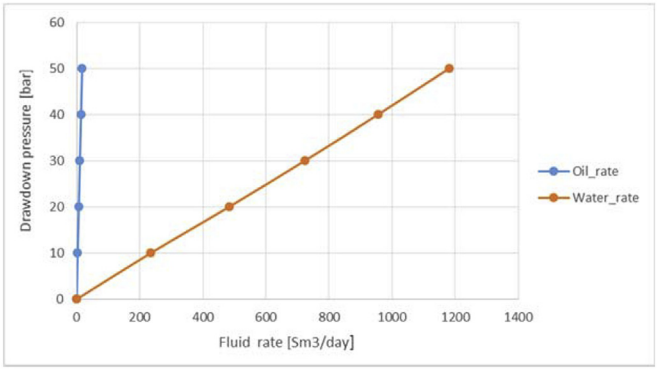

Fig. 12. Total production rates as a function of the drawdown pressure for a 20 mm ICD.

production when changing the well completion from ICD to AICV in a field with CO_2 injection. Fig. 11 and Fig. 12 show the total production rates for the gridless reservoir cases using the tuned AICV model and passive ICD respectively. The drawdown ($P_{Reservoir}$-P_{well}) is varied from 10 to 50 bar and since oil is only produced in zone M1 and M2, the total production rate of oil is the same for the two cases. However, the ICDs are not able to choke for water, resulting in a very high water production when the drawdown is increased. Therefore, if passive ICD with 2 bar strength is used, the total production has to be choked which again results in a low oil production rate. The AICV chokes the zone with high water production, which reduces the water production rate drastically and the well can thereby be run with a high drawdown. When using ICD, the oil flow rate is 3.4 m^3/day (21.4 bopd) and the total liquid flow rate is 238 m^3/day (1500 bpd) at 10 bar drawdown, which gives a WC of 98.3%. By using AICV and increasing the drawdown to 50 bar, the oil production can be increased from 3.4 m^3/day (21.4 bopd) to 17.4 m^3/day (110 bpd). The water production at 50 bar is 32 m^3/day, which gives a water cut of 65% under these conditions.

The further simulations are performed with AICV completion and 50 bar drawdown. Six AICVs, two in each production zone, are implemented in the vertical well. Packers are installed between each zone. Fig. 13 presents the well with AICVs and packers. M1, M2 and M3 indicates where the different zones are located, and by comparing Fig. 13 with Fig. 8, M3 is the lower zone, M2 is the middle zone and M1 is the upper zone. The oil and water production rates together with the water cut (WC) as a function of vertical position are presented in Fig. 14. The volume flow rates per meter well are presented in Sm^3/day/m. As can be seen from the figure, oil is produced in zone M1 and M2 and the water production occurs in zone M3 only. The water saturation in zone M3 was set to 100%, giving a WC of 100% in that zone. Fig. 15 shows the cumulative oil and water production rates in Sm^3/day. The flow rates of oil and water are 17.4 Sm^3/day (110 bopd) and 32.0 Sm^3/day (200 bopd) respectively, and the water cut is 65%. The simulated results predict the potential of increased oil recovery with AICV completion. The oil production increased with 410% and the water cut was decreased significantly. Since it is assumed that the CO_2 is solved in water (carbonated water), this indicates that recirculation of CO_2 is also reduced significantly. If the CO_2 reaches the well as CO_2 gas or supercritical CO_2, the AICV is designed to also close for CO_2 under these conditions. Reports from the trial well state that the GOR before recompletion was high, and that the high GOR was mainly due to reproduced CO_2 (Kais et al., 2016). However, the GOR is given at standard conditions (Sm^3 gas/Sm^3 oil), which may involve that the CO_2 was solved in liquid (oil and water) at the reservoir conditions.

Comparison of simulation data and production data from the Midale field is presented in Table 4. The simulations were only run with water and oil, and the GOR is therefore not included in the table. AICV completion gives the highest oil production and lowest water production. The reason is that AICV chokes or closes for water and a higher drawdown can be used without increasing the total liquid flow dramatically. ICD and “open hole” produce more water than what can be handled by the topside separation system. The simulations show the potential for the AICV at high drawdown. In the trial well, the bottom plug was damaged when the drawdown reached 50 bar. Due to this, the water in M3 bypassed the AICV in M3 and large amount of water was flowing through the damaged plug. When the AICV chokes for water in a zone, large differential pressure can be created over the completion, and the packers and bottom plug have to be constructed to withstand this high pressure difference. The bottom plug in the trial well was not designed for these high pressure differences, and the plug was damaged. When a large quantity of water was freely flowing through the damaged plug, the consequence was that the drawdown in zone M1 and M2 is reduced and the oil production from these zones decreases. This shows that packers, plugs and other completing equipment need to withstand a higher differential pressure in an AICV well than in a standard ICD well. Fig. 16 shows an illustration of the production from the original open hole well compared to the simulated AICV well with the bottom plug is intact. Using AICV, the water flow (blue arrow) is reduced significantly, and the oil rates (black arrows) are increased. In Fig. 17, the open hole case is compared to the AICV trial well with the damaged plug. It can be seen that the water (blue arrow) from M3 bypasses the choked AICV and flows directly into the base pipe through the damaged plug. The oil production with AICV has increased compared to the open hole case.

The oil production rate from the AICV pilot well corresponds to the simulated oil production at 20 bar drawdown. Due to the high flow rate of water, the drawdown in M1 and M2 can have been reduced to 20 bar,

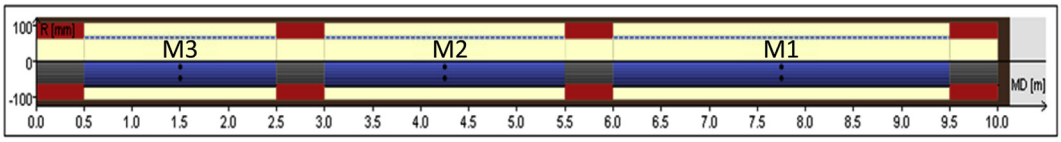

Fig. 13. Sketch of the production well including six AICVs (black dots) and four packers (red rectangles). (For interpretation of the references to colour in this figure legend, the reader is referred to the Web version of this article.)

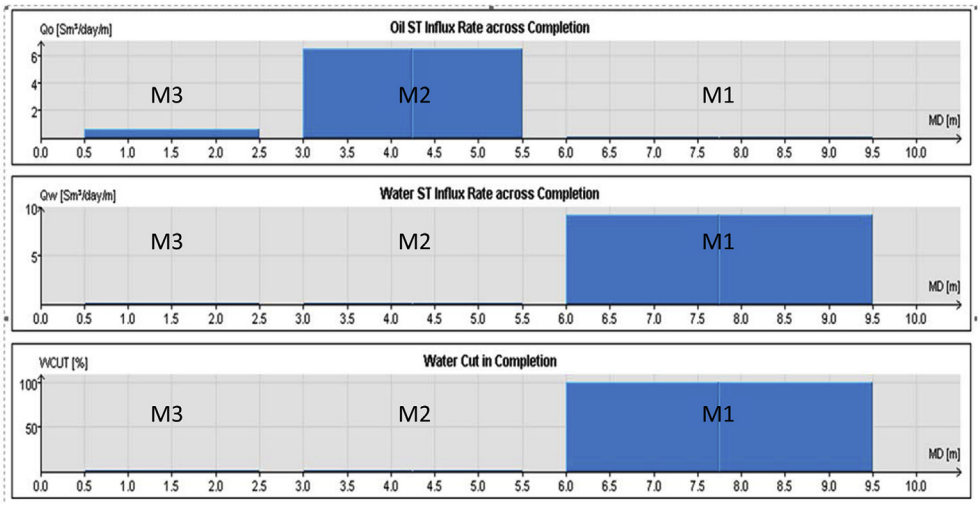

Fig. 14. Oil and water influx rate [Sm^3/day/m] and water cut [%] as a function of position.

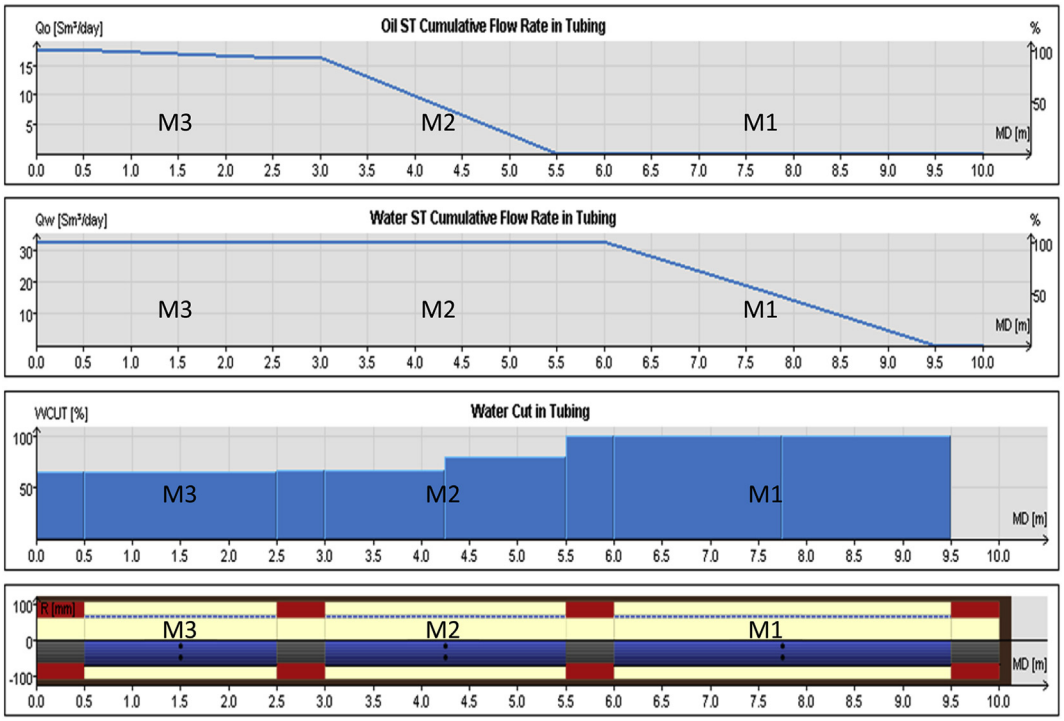

Fig. 15. Water cut and cumulative oil and water flow rates in the pipeline.

Table 4
Comparison of production data and simulation results.

	Production data				Simulations			
	Drawdown	Oil [bopd]	Liquid [bpd]	WC [%]	Drawdown	Oil [bopd]	Liquid [bpd]	WC [%]
Open hole	< 5 bar	5	1100	99.6				
ICD					10 bar	21.4	1520	98.6
ICD	≈20–50 bar	45	3500	98.7	50 bar	110	7530	98.5
AICV					10 bar	21.4	135	84.1
AICV	≈20–50 bar	39	3100	98.5	50 bar	110	310	65

which gives a good agreement between simulations and production data. This indicates that NETool is able give a good prediction of the production results from the trial well, and can be used to study the potential of increased oil recovery with AICV in fields utilizing CO_2-EOR.

6. Conclusion

A vertical well in the Midale carbonate field was selected as a trial well for evaluating the benefit of using autonomous inflow controls in combination with CO_2 EOR. The production data from the original well

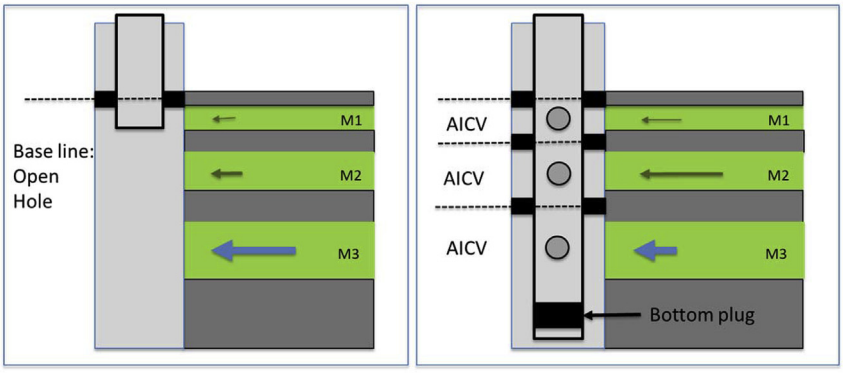

Fig. 16. Illustration of the flow from the different layers. Comparison between open hole production and AICV simulation.

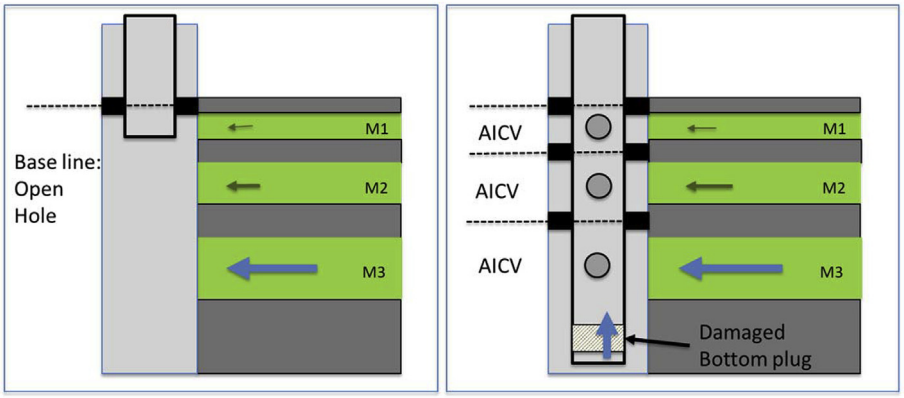

Fig. 17. Illustration of the flow from the different layers. Comparison between open hole and AICV production from field test.

with open-hole completion are compared with the production data obtained using AICV wells. Based on the production data it was found that AICV has the ability to autonomously sense unwanted fluids and then choke their flow until wanted fluids migrate back to the wellbore. This is a significant advantage over a passive inflow control. AICV can be designed for a wide range of fluid properties. The tests with AICVs showed significant increase in oil production and reduced the water cut and gas oil ratio. The oil rate increased with 690%. The water cut was still high due to leakage through a damaged plug. The high water flow through the damaged plug also resulted in reduced drawdown and production in the oil producing zones. AICV completed wells can be run with high drawdown, which results in increased oil production.

Simulations were performed with NETool, which is a steady state one dimensional near well simulation tool. Simulations were run using the trial well data and the reservoir conditions from the Midale field. An autonomous inflow control model implemented in NETool was tuned to fit the performance curves for the AICV. Relative permeability curves for carbonate reservoirs was estimated and implemented in NETool. Simulations were performed with passive ICD and AICV. The results indicate that the oil production can be increased with more than 400% when AICV is used at high drawdown. ICD cannot choke locally for water or CO_2, and is producing very high amount of unwanted fluids at high drawdown. The water cut using AICV is 65% at 50 bar drawdown whereas the water cut is close to 100% when using ICD. NETool was able to predict the potential of increased oil recovery with AICV completion.

Acknowledgement

The authors will like to give a special thanks to Gassnova Climit for supporting and funding the project “Autonomous valves for increased oil recovery and CO_2 storage. Without the funding from Gassnova Climit, it would not be possible for InflowControl to be present in Midale field to follow up the installation and production. We will also like to thank Apache for leading the project and allowing the results to be published.

References

Aakre, Haavard, Halvorsen, Britt, Werswick, Bjørnar, Mathiesen, Vidar, 2013a. Smart well with autonomous inflow control valve technology. In: SPE 164348-MS. Paper Presented at the SPE Middle East Oil and Gas Show and Exhibition, Manama, Bahrain, 10–13 March 2013.

Aakre, Haavard, Halvorsen, Britt, Werswick, Bjørnar, Mathiesen, Vidar, 2013b. Increased oil recovery of an old well, recompleted with Autonomous Inflow Control Valve (AICV). In: Paper Presented at the ADIPEC 2013 Technical Conference, Abu Dhabi, 10–13 November 2013.

Aakre, H., Halvorsen, B.M., Werswick, B., Mathiesen, V., 2014. Autonomous inflow control valve for heavy and extra-heavy oil. In: SPE171141, SPE Heavy and Extra Heavy Oil Conference, Latin America, Medellin, Colombia, 24-26 September, 2014.

http://dwsim.inforside.com.br/wiki/index.php?title=Black-Oil_Simulations.

Ghoodjani, E., Bolouri, S.H., 2011. Experimental Study and Calculation of CO2-oil Relative Permeability. 53-(2). (1337-7027)Petroleum & Coal Sharif University of Technology and Shahid Bahonar University, Iran, pp. 123–131.

Halvorsen, Martin, Elseth, Geir, Magne Nøvdal, Olav, 2012. Increased Oil Production at Troll by Autonomous Inflow Control with RCP. SPE 159634. .

Halvorsen (Statoil), Martin, Madsen (Statoil), Martin, Vikøren Mo (Statoil), Mathias, Isma Mohd (Tendeka), Ismail, Green (Tendeka), Annabel, 2016. Enhanced Oil Recovery on Troll Field by Implementing Autonomous Inflow Control Device. SPE-180037-MS Society of Petroleum Engineers.

Kais, Ransis, Mathiesen, Vidar, Aakre, Haavard, Woiceshyn, Glenn, 2016. First autonomous inflow control valve (AICV) well completion deployed in a field under an EOR (water & CO2 injection) scheme. In: SPE-181552-MS, SPE Annual Technical Conference and Exhibition Held in Dubai, UAE, 26–28 September 2016.

Mathiesen, Vidar, Aakre, Haavard, Werswick, Bjørnar, Elseth, Geir, Statoil, A.S.A., 2011. The Autonomous RCP Valve-new Technology for Inflow Control in Horizontal Wells. SPE 145737. .

Mathiesen, V., Aakre, H., Werswick, B., 2014. The Next Generation Inflow Control-the Next Step to Increase Oil Recovery on the Norwegian Continental Shelf. SPE 169233. .

NETool™ FundamentalsRelease 5000.0.4.0, Halliburton, 2015. NETool Fundamentals Release 5000.0.2.0-cloudapp.net.

Optimization of CO2 Storage in CO2 Enhanced Oil Recovery Projects, Advanced Resources International and Melze Consultin. http://neori.org/resources-on-co2-eor/how-co2-eor-works/November2010.
Schneider, F.N., Owens, W.W., 1970. Sandstone and carbonate two- and three-phase relative permeability characteristics. Trans. AIME 249, 75–84.
Tiab, Djebbar, Donaldson, Erle C., 2012. Petrophysics, Theory and Practice of Measuring Reservoir Rock and Fluid Transport Properties, third ed. Gulf Professional Publishing, USA978-0-12-383848-3.
U.S. Department of Energy, 26 November 2015. Enhanced Oil Recovery. http://energy.gov/fe/science-innovation/oil-gas-research/enhanced-oil-recovery.
Zhang, L., Ren, B., Huang, H., Li, Y., Ren, S., Chen, G., et al., 2015. CO2 EOR and storage in Jilin oilfield China: monitoring program and preliminary results. J. Pet. Sci. Eng. 125, 1–12.